CHAPTER 16

Mechanosensitive Ion Channels in Dystrophic Muscle

Jeffry B. Lansman
Department of Cellular and Molecular Pharmacology,
School of Medicine, University of California, San Francisco, California 94143

I. Overview
II. Introduction
III. MS Channel Expression During Myogenesis
IV. Permeabilty Properties of MS Channels in Skeletal Muscle
  A. Permeability to Monovalent Cations
  B. Permeability to Divalent Cations
V. Gating
  A. SA Gating
  B. Voltage-Sensitive Gating
  C. Modal Gating in *mdx* Muscle
VI. Pharmacology
  A. Block by Gadolinium Ion
  B. Aminoglycoside Antibiotics
VII. Conclusions
  References

I. OVERVIEW

Mechanosensitive (MS) ion channels are expressed abundantly in skeletal muscle at all stages of development. In wild-type muscle, MS channels show primarily stretch-activated (SA) gating. In dystrophic myotubes from the *mdx* mouse, a loss-of-function mutant that lacks dystrophin, there are two types of MS channels. In addition to conventional SA channels, some channels shift into a novel gating mode in which channels stay open for extended periods of time and are stretch-inactivated (SI). The shift in gating

Current Topics in Membranes, Volume 59
1063-5823/07 $35.00

DOI: 10.1016/S1063-5823(06)59017-9

mode can occur slowly at the start of an experiment or more abruptly in response to strong pressure or voltage steps. SA and SI gating have similar energetic requirements which likely reflect the energy required to deform the bilayer. The pharmacological properties of MS channels show similarities to other cation-selective channels. Highly charged pharmacological probes such as lanthanide cations and aminoglycoside antibiotics act by plugging the channel pore rather than interacting with the lipid bilayer.

II. INTRODUCTION

The ability to detect mechanical forces is shared by all living organisms. Mechanical sensitivity underlies the detection of auditory and tactile stimuli as well as distension pressures, shear stresses, and osmotic gradients in various cell types. Despite the importance of mechanical sensitivity, it remains the least understood sensory process. MS ion channels are thought to constitute primary sensors of mechanical stimuli. In most cases, however, their molecular identity and mechanism of force transduction remain largely unknown.

SA MS channels were first detected in skeletal muscle cells using single-channel recording methods (Brehm *et al.*, 1984; Guharay and Sachs, 1984). Guharay and Sachs (1984) found that treating cells with drugs that disrupt actin filaments or microtubules increased the sensitivity of SA channels to membrane tension. This finding suggested a role of the cytoskeleton in transduction of membrane tension. Skeletal muscle possesses a complex cytoskeleton that plays a key role in maintaining its shape and surface morphology, as well as supporting stresses generated during contraction. How cytoskeletal structures regulate mechanotransduction has been a difficult question to address experimentally. One approach to this problem is to use loss-of-function mutants in which a specific cytoskeletal protein is absent.

Dystrophin is a large submembrane cytoskeletal protein that is a member of the β-spectrin/α-actinin protein family (Koenig *et al.*, 1988). Dystrophin is linked to the membrane by a glycoprotein complex composed of the sarcoglycans, dystroglycan, syntrophin, and dystrobrevin (Ervasti *et al.*, 1990; Yoshida and Ozawa, 1990; Ibraghimov-Beskrovnaya *et al.*, 1992, 1993; Adams *et al.*, 1993; Ahn *et al.*, 1996). The glycoprotein complex spans the membrane and connects the actin cytoskeleton to laminin in the extracellular basement membrane (Ervasti and Campbell, 1993). In the *mdx* mouse, a point mutation in exon 23 of the dystrophin gene leads to the loss of full-length dystrophin in skeletal muscle (Hoffman *et al.*, 1987; Sicinski *et al.*, 1989). The *mdx* mouse model makes it possible to study the biophysical consequences of the loss of dystrophin on the mechanotransduction process.

III. MS CHANNEL EXPRESSION DURING MYOGENESIS

During myogenesis, myoblastic stem cells differentiate and form multinucleated skeletal muscle cells (Fig. 1A). *In vitro*, myoblasts proliferate until stimulated to withdraw from the cell cycle and begin differentiation. Subsequently, myoblasts align oriented with their long axis in parallel and fuse to

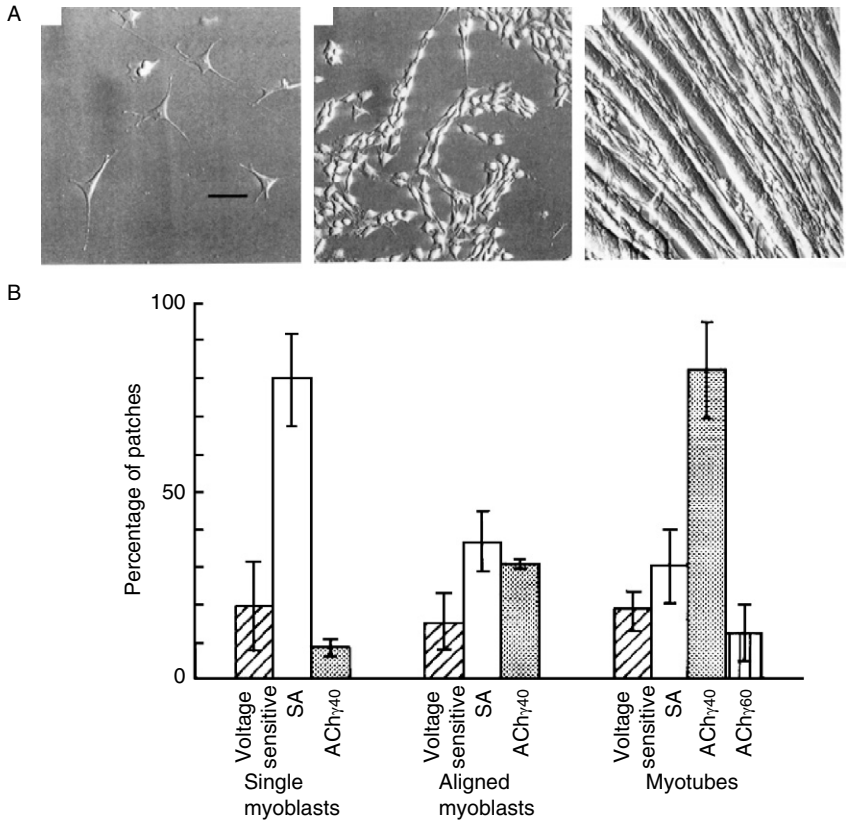

FIGURE 1 Expression of MS channels during myogenesis. (A) Micrograph showing the stages of myogenesis *in vitro* during which patch clamp recordings were made: single myoblasts ~24 h after plating C2 mouse muscle cells at low density (left); myoblasts that had proliferated in culture and had aligned prior to fusion (middle); and multinucleated myotubes during the first week after myoblast fusion (right). (B) Fraction of patches containing the acetylcholine receptor channel, SA channel, and a voltage-insensitive cation channel. $ACh_{\gamma 40}$ and $ACh_{\gamma 60}$ represent the small and large conductance acetylcholine receptor channels, respectively. $ACh_{\gamma 60}$ is the adult form of the AChR channel that appears in fully differentiated muscle fibers. Adapted from Franco and Lansman (1990a).

form electrically excitable multinucleated myotubes. Figure 1B shows that MS channels can be detected at all stages of myogenesis *in vitro*. SA MS channels are highly expressed in myoblasts (~80% patches) but expression declines during skeletal muscle differentiation (~30% patches in myotubes). In all of the recordings, ~15–20 patches contained activity of a cation-selective channel that showed an increase in open probability with membrane depolarization, but was otherwise insensitive to membrane stretch. This activity was originally thought to represent MS channels in patches where membrane geometry prevented normal force transduction. More recent data suggests this activity arises from a cation channel regulated by IGF-1 (unpublished data).

IV. PERMEABILTY PROPERTIES OF MS CHANNELS IN SKELETAL MUSCLE

A. Permeability to Monovalent Cations

MS channels in skeletal muscle are permeable to monovalent cations, but show rather low selectivity among the alkali metal cations. MS channel currents are well resolved when extracellular Na^+ is replaced with 155-mM Li^+, Na^+, K^+, Rb^+, or Cs^+. The single-channel conductance is largest with Rb^+ as the charge carrier (~38 pS) and smallest with Li^+ (~27 pS); (Franco and Lansman, 1990a). The conductance selectivity sequence is Rb > K > Na > Cs > Li, which corresponds to Eisenman sequence III for a weak field strength site (Eisenman, 1962). There is little change in the reversal potential in the presence of the different alkali cations, indicating little discrimination among the alkali metal cations.

B. Permeability to Divalent Cations

MS channels in skeletal muscle have a relatively high permeability to Ca^{2+} and other divalent cations. Figure 2 shows records of the activity of single MS channels in the presence of Ca^{2+}- or Ba^{2+}-containing solution. The single-channel current–voltage relation in the presence of either 110-mM Ca^{2+} or 110-mM Ba^{2+} as the extracellular solution gives single-channel conductances of ~13 and 24 pS, respectively. The reversal potential in the presence of Ca^{2+}-containing solutions (+22 mV) was used to calculate the relative permeability of Ca^{2+} to K^+ (P_{Ca}/P_K), which was ~7. MS channels in skeletal muscle, thus, have a relatively high permeability to Ca^{2+}. The high Ca^{2+} permeability allows relatively large Ca^{2+} fluxes at negative membrane potentials.

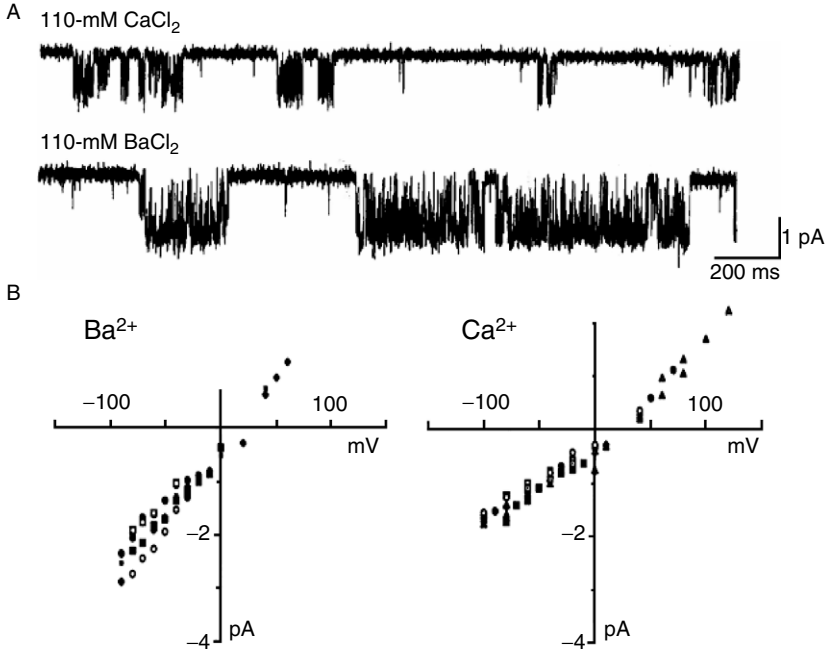

FIGURE 2 Ca^{2+} permeability of MS channels in skeletal muscle. (A) Single-channel currents carried by Ca^{2+} (top) or Ba^{2+} (bottom). The holding potential was −60 mV. The patch electrode contained either 110-mM $CaCl_2$ or $BaCl_2$. (B) The single-channel current–voltage relation. Filled symbols, recordings from cultured myotubes; open symbols, recordings from myoblasts. Different symbols represent recordings from different patches. The conductance was 13.1 ± 1 pS and current reversed at +22 ± 6 mV (S.D., $n = 8$) with Ca^{2+}; the conductance was 24 ± 4 pS and current reversed at +17 ± 8 mV (S.D., $n = 7$) with Ba^{2+}. Adapted from Franco and Lansman (1990a).

V. GATING

A. SA Gating

SA MS channels are found in myotubes grown in tissue culture (Franco and Lansman, 1990a; Franco-Obregón and Lansman, 1994). SA with identical conductance properties can also be detected in skeletal muscle fibers acutely isolated from the flexor digitorum brevis (FDB), a small, fast twitch fiber (Franco-Obregón and Lansman, 1994). Patch clamp recordings from FDB fibers from 2-week-old mice show that ~70% patches contain SA channels, although these have a much lower resting open probability in the absence of a pressure stimulus. Despite these differences, SA channels in

myotubes and fibers in wild-type muscle activate over a similar pressure range in response to either positive or negative pressure.

The absence of dystrophin in *mdx* FDB fibers alters the pressure sensitivity of SA channels. Figure 3 shows the activity of SA channels recorded from FDB fibers from wild-type (Fig. 3A) or *mdx* (Fig. 3B) mice. In both cases, channel activity increases on applying negative pressure to the electrode. Figure 3C shows the pressure dependence of channel opening. Channel opening was somewhat less sensitive to pressure in *mdx* fibers. In addition, channel activity after a step of negative pressure in recordings from *mdx* fibers was generally smaller than the activity before the pressure step (data not shown, see Franco-Obregón and Lansman, 1994). By contrast, channel activity was higher after a pressure step compared with activity before the step in wild-type fibers. These differences in SA gating may reflect differences in the

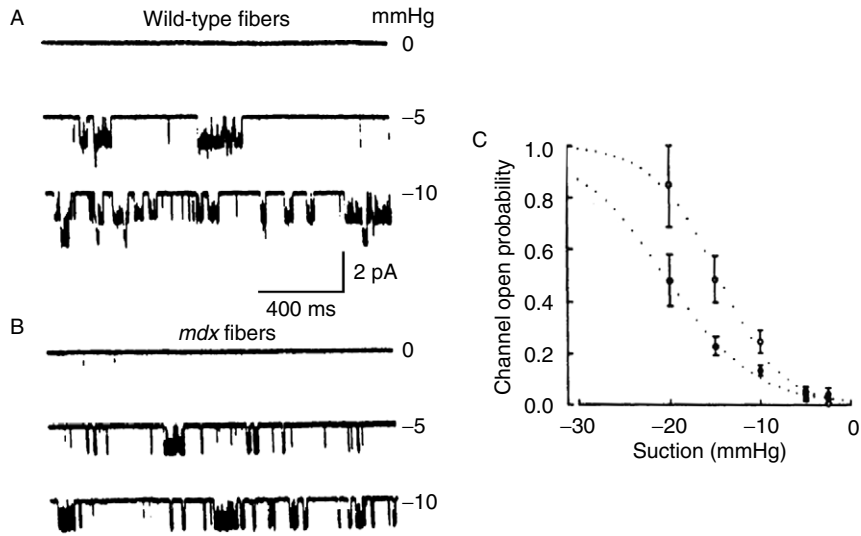

FIGURE 3 SA channels in acutely isolated wild-type and *mdx* FDB fibers. (A) Single-channel activity recorded from wild-type FDB fiber. Pressure applied to the electrode is indicated to the right of each current record. (B) Single-channel activity recorded from an *mdx* FDB fiber. (C) The relationship between pressure and channel open probability. Recordings were made from wild-type (open symbols; $n = 22$) and *mdx* (filled symbols; $n = 25$) FDB fibers. The fit through the experimental points represent the Boltzmann relationship with half-activation pressure, $P_{1/2}$ of -14.0 and -20.0 mmHg and steepnesses -3.0 and -5.0 mmHg, for wild-type and *mdx* fibers, respectively. FDB fibers were isolated from 2-week-old mice. At this age, 17% of the recordings from wild-type and 22% of the recordings from *mdx* fibers had cation channel activity that failed to respond to suction. Adapted from Franco-Obregón and Lansman (1994).

mechanical properties of the membrane of wild-type and *mdx* muscle (Pasternak *et al.*, 1995).

B. Voltage-Sensitive Gating

SA channels in skeletal muscle have a voltage-sensitive gating mechanism in which channel burst duration increases with depolarization (Franco and Lansman, 1990). This is shown for the SA channels in FDB fibers in Fig. 4A. Figure 4B shows that channel open probability increases with membrane depolarization, but the intrinsic voltage sensitivity is similar for MS channels in wild-type (open symbols) and *mdx* (filled symbols) fibers. It is interesting that SA channels in wild-type and *mdx* fibers have different sensitivities to stretch, but not to voltage. A simple explanation for this is that differences in sensitivity to membrane stretch reflect differences in the mechanical properties of the membrane of dystrophin-containing and dystrophin-deficient muscle. Voltage sensitivity, on the other hand, is apparently unaffected by the presence or absence of dystrophin, suggesting there is a direct effect of voltage on channel gating that does not depend on membrane mechanics.

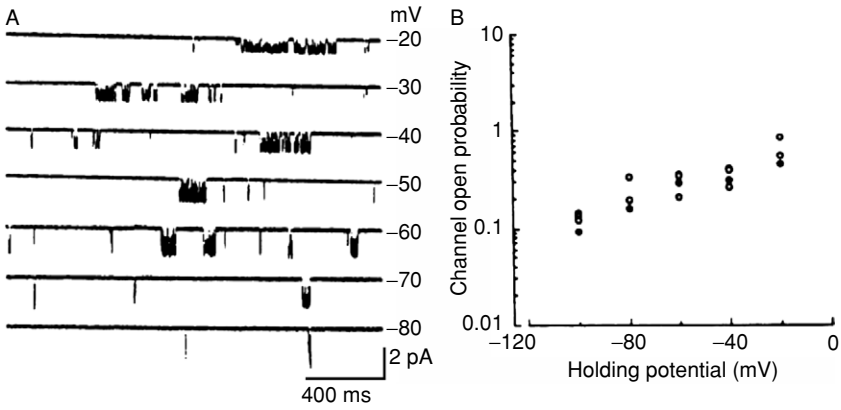

FIGURE 4 Voltage-dependent gating of SA channels. (A) Records of single-channel activity obtained from a recording on an *mdx* FDB fiber. The patch holding potential is indicated at the right of each current record. (B) Effect of the holding potential on channel open probability in recordings from wild-type (open symbols) and *mdx* (filled symbols) fibers. Channel activity increased with depolarization ~*e*-fold per 56 and 53 mV in wild-type and *mdx* fibers, respectively.

C. *Modal Gating in* mdx *Muscle*

1. SI Gating Mode

Patch clamp recordings from tissue cultured myotubes from *mdx* mice have revealed striking changes in MS channel behavior that cannot be explained in terms of simple changes in membrane mechanical properties associated with dystrophin deficiency (Franco and Lansman, 1990b, 2002). MS channels typically are open for only a few milliseconds at rest and a pressure stimulus causes stretch activation. In some recordings from *mdx* myotubes (~20–50% patches), however, MS channels remain open for many tens of seconds. The persistent opening of MS channels has been interpreted as a shift in gating mode where the open state is energetically favored at rest. Figure 5 shows an example of a change in MS channel gating mode that occurred at the start of an experiment. In *mdx* muscle, MS channel open probability was low at the start of the recording, but gradually increased over the next several minutes (Fig. 5A). Channels remained open almost continuously for the duration of the experiment. By contrast, MS channels in wild-type myotubes open only very briefly at the beginning of the recording but then close and remain closed (Fig. 5B).

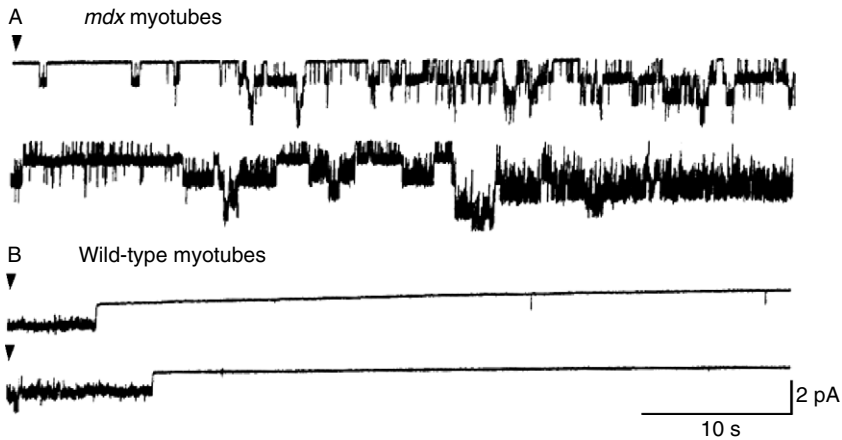

FIGURE 5 A novel MS channel gating mode characterized by persistent channel opening in *mdx* myotubes. (A) Recording from a patch on an *mdx* myotube showing a slow, persistent increase in channel opening following the start of the recording (arrowhead). (B) Recordings from two different wild-type myotubes showing that seal formation (arrowhead) caused a brief inward current, but channel activity remained negligible for the duration of the recording in the absence of a pressure stimulus. Single-channel currents were filtered at 0.5 kHz and sampled at 1.25 kHz. Adapted from Franco-Obregón and Lansman (2002).

MS channels that become persistently open also acquire a SI gating mechanism. Figure 6A shows the open probability measured during consecutive sweeps plotted as a function of time during the experiment that lasted for about 10 min. Applying negative pressure suppressed channel activity. Figure 6B shows representative currents during an individual sweep with either 0-mm applied pressure (first and third traces) or −30 mmHg (second and fourth traces). The data show that SI gating is readily reversible and quite stable over many minutes.

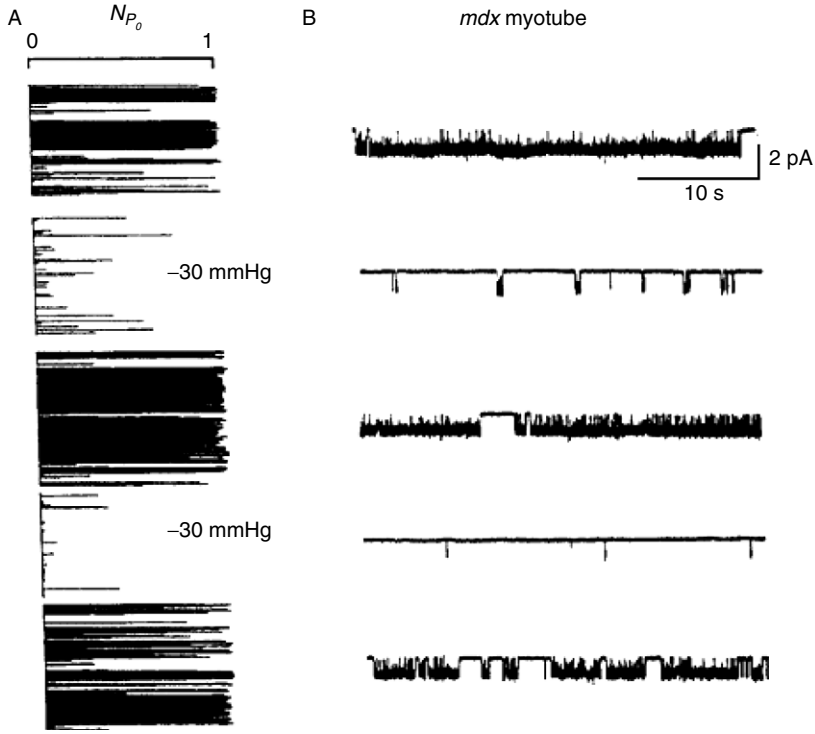

FIGURE 6 The SI gating mode. (A) MS channel open probability (Np_o) during consecutive 1 s intervals of a recording lasting ~13 min. This patch contained only a single channel. Suction was applied to the patch electrode at the indicated times. Mean channel open probability during the first 143-s interval was 0.54, and applying −30 mmHg of pressure to the electrode for 153 s reduced channel open probability to 0.044. After releasing the pressure, channel open probability returned to 0.85 and a subsequent application of −30 mmHg for 137 s reduced channel open probability to 0.01; open probability returned to 0.63 after suction was released. (B) Representative current records during the indicated periods. Single-channel currents were filtered at 0.5 kHz and sampled at 1.25 kHz. Adapted from Franco-Obregón and Lansman (2002).

An analysis of the pressure dependence of SA and SI showed an important similarity in the transduction process, despite the fact that pressure causes opposite changes in channel opening. Figure 7 shows the relationship between pressure and channel open probability for SA (left) and SI channels (right). The data were fit with a Boltzmann relation with half-maximal activation pressures $P_{1/2}$ of −36.5 and −13 mmHg and steepnesses −6 and −6.5 for SA and SI channels, respectively. Although, stretch-inactivation is shifted to more negative pressures compared with stretch-activation, the slopes of the Boltzmann fit are similar. This suggests that both types of gating involve a single energetic process, such as thinning of the lipid membrane adjacent to the channel during membrane deformation (see Section VII).

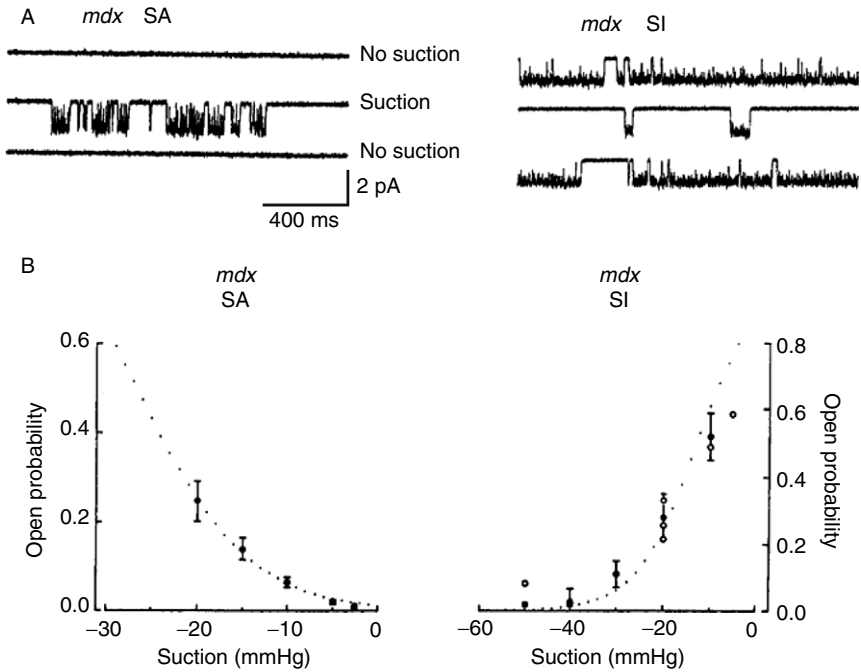

FIGURE 7 Pressure dependence of SA and SI gating. (A) Single-channel currents showing SA (left) and SI (right) mechanotransduction modes. Recordings made with standard saline in the patch electrode. Top records, channel activity in the absence of applied pressure; middle records, after applying −15 mmHg suction to the electrode; bottom records, after releasing the pressure stimulus to 0 mmHg. (B) Relationship between the pipette pressure and channel open probability for SA (left, $n = 6$) and SI channels (right, $n = 14$). Data were fit with a Boltzmann relation with half-maximal activation pressures $P_{1/2}$ of −36.5 and −13 mmHg and steepnesses −6 and −6.5 for SA and SI channels, respectively. Adapted from Franco-Obregón and Lansman (2002).

2. Stretch-Induced Gating Mode Transitions

The hypothesis that SA and SI gating represent two gating modes of a single type of MS channel was strengthened by the finding that membrane stretch was a sufficient stimulus to cause conversion between the two gating modes. The transition always involved a shift from SA to SI gating and was essentially irreversible over the time course of the recording. Figure 8 (top)

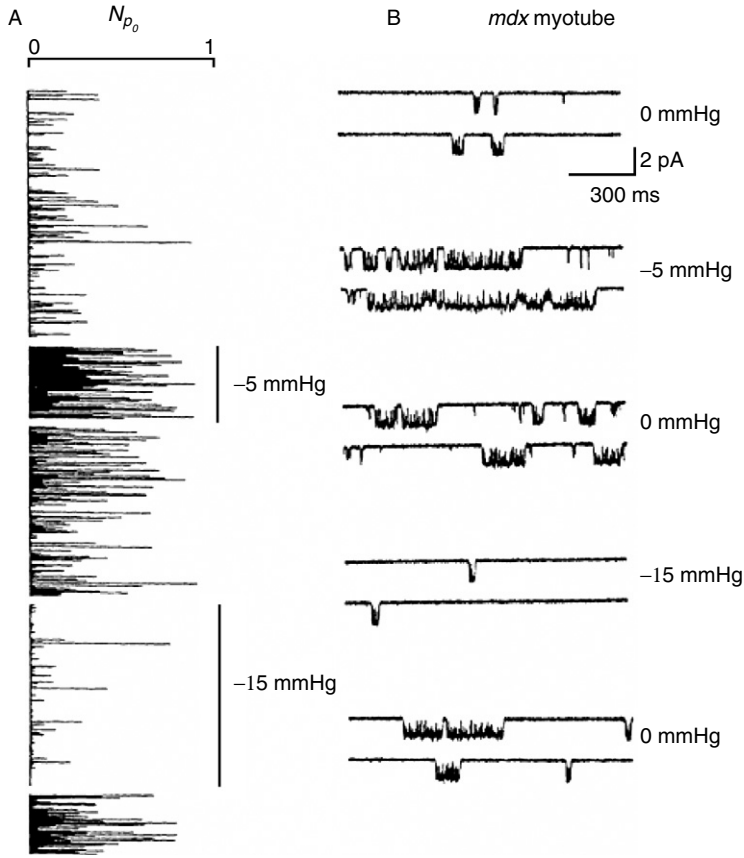

FIGURE 8 Induction of the SI gating mode by membrane stretch. (A) Channel open probability (Np_o) measured in consecutive 300-ms sweeps. The bars indicate the time during which the indicated pressure stimulus was applied to the patch electrode. (B) Representative current records obtained during the experiment. $Np_o = 0.04$ at the beginning of the experiment, 0.20 after applying −5mmHg of suction, 0.15 after subsequently releasing the pressure stimulus, 0.01 after application of a second suction stimulus of −15mmHg, and 0.10 after releasing the pressure stimulus. Adapted from Franco-Obregón and Lansman (2002).

shows an example of a stretch-induced transition in MS channel gating mode. Figure 8A shows a plot of channel open probability for consecutive ~1-s sweeps lasting for the entire recording which lasted ~10 min. The plot of open probability vs time during the experiment shows that the response of an MS channel to membrane stretch changed. This is seen more clearly in the records in Fig. 8B. For example, applying suction initially increased channel opening (Fig. 8B, second pair, −5 mmHg) and channels remained open. When suction was applied for a second time, channels closed as is characteristic of SI gating.

VI. PHARMACOLOGY

A. Block by Gadolinium Ion

The lanthanide Gd^{3+} has an ionic radius of 0.105 nm, close to Ca^{2+} with an ionic radius of 0.106 nm, and is useful as a transition state analogue for studying Ca^{2+}-binding sites in ion channels and other proteins. Gd^{3+} blocks SA channels with high affinity (Yang and Sachs, 1989; Franco and Lansman, 1990) but the mechanism of block is not well understood. Gd^{3+} binds to charged phospholipids with high affinity and produces strong electrostatic effects that modify bilayer properties (Ermakov *et al.*, 1998). This has suggested that Gd^{3+} inhibits MS channels by its effects on lipids rather than by binding to the MS channel pore. However, an analysis of the block of persistently open SI channels in *mdx* muscle by Gd^{3+} indicates that it acts by simply plugging the open channel thereby preventing ion flow (Franco *et al.*, 1991).

Figure 9 shows Gd^{3+} block of high p_o MS channels in *mdx* myotubes. Entry and exit of Gd^{3+} from the open channel is resolved as the discrete interruptions of the single-channel current. As expected for a simple bimolecular reaction between a single Gd^{3+} ion and a site in the open channel, increasing the concentration of Gd^{3+} increased the number of interruptions of the single-channel current (Fig. 9B). Measurements of the durations of the open and blocked times showed Gd^{3+} entry into the channel (blocking rate) is insensitive to membrane potential, while Gd^{3+} exit from the pore (unlocking rate) is faster at negative potentials. An increased rate of unblocking with hyperpolarization indicates Gd^{3+} binds within the channel and is swept into the cell interior at negative voltages where the applied electric field exceeds the chemical binding energy.

If Gd^{3+} acts within the lipid bilayer to modify channel gating, then it would be expected to change the pressure sensitivity of channel opening, reflecting a mechanism of inhibition at the level of the mechanotransduction process. Measurements were made of the pressure-open probability relation for SI channels in the presence of Gd^{3+}. The Boltzmann parameters used to

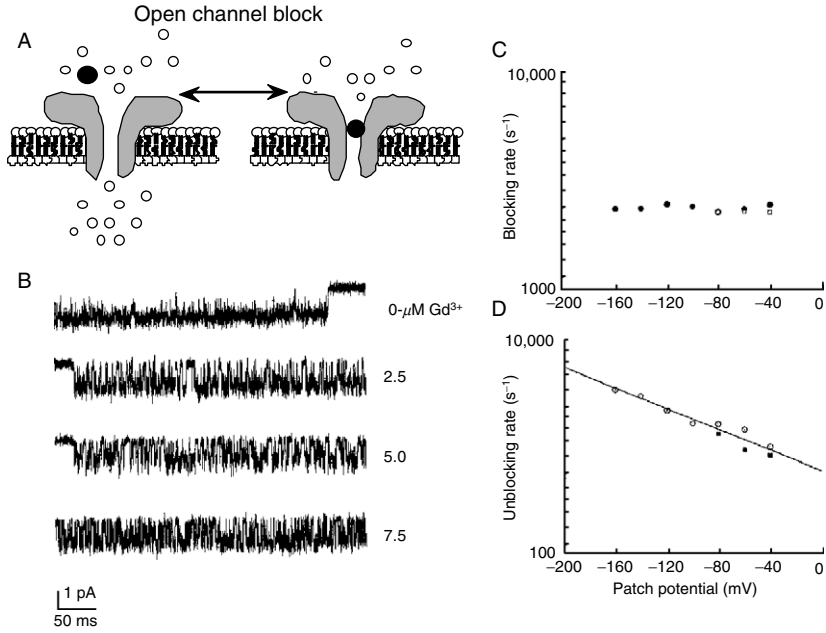

FIGURE 9 Gadolinium block of MS channels. (A) Illustration showing the open channel blocking model. Gd^{3+} is present in the extracellular solution at a low concentration. The right figure shows an open channel that is freely permeable to Na^+ and Ca^{2+} in the extracellular solution (open circles). Binding of the blocking ion to a site in the channel prevents ion conduction by physically occluding the channel permeation pathway. (B) Single-channel currents recorded from *mdx* myotubes with electrodes containing physiological saline and the indicated concentration of Gd^{3+}. The holding potential was −60 mV. Currents were filtered at 2 kHz. (C) Dependence of the blocking rate on the patch potential. Open symbols represent the inverse of the mean open time (blocking rate) obtained from a single exponential fit to the histograms of open times. Filled symbols are obtained from an analysis of the distribution of current amplitudes. (D) Dependence of the unblocking rate on the patch potential. Filled squares represent the inverse of the mean blocked time obtained from the exponential fit to the histogram of closed times. Open circles are obtained from an analysis of the distribution of current amplitudes. The line through the experimental points is the fit to a single exponential. The unblocking rate changed ~*e*-fold per 85 mV, which corresponds to an effective electrical distance $\delta = 0.09$ for a trivalent blocking particle. Adapted from Franco *et al.* (1991).

fit the pressure-open probability curve for the SI channel in the presence of Gd^{3+} ($P_{1/2} = -17$ mmHg and steepness = 6 mmHg) were virtually the same as the *mdx* SI channels in the absence of blocker (see above). It is likely that Gd^{3+} exerts its blocking actions within the MS channel pore and, apparently, does not alter the properties of the bilayer sufficiently to alter mechanotransduction.

B. Aminoglycoside Antibiotics

Aminoglycoside antibiotics are positively charged molecules that interact with both membrane lipids and ion-binding sites of proteins. In skeletal muscle, aminoglycosides block both the L-type channel and MS channel (Haws *et al.*, 1996; Winegar *et al.*, 1996). Block of MS channels occurs in the submillimolar range ($K_D = \sim 200\ \mu M$ for neomycin at pH 7.4) and involves a partial occlusion of the channel pore at high concentrations. Figure 10 shows the partial block of

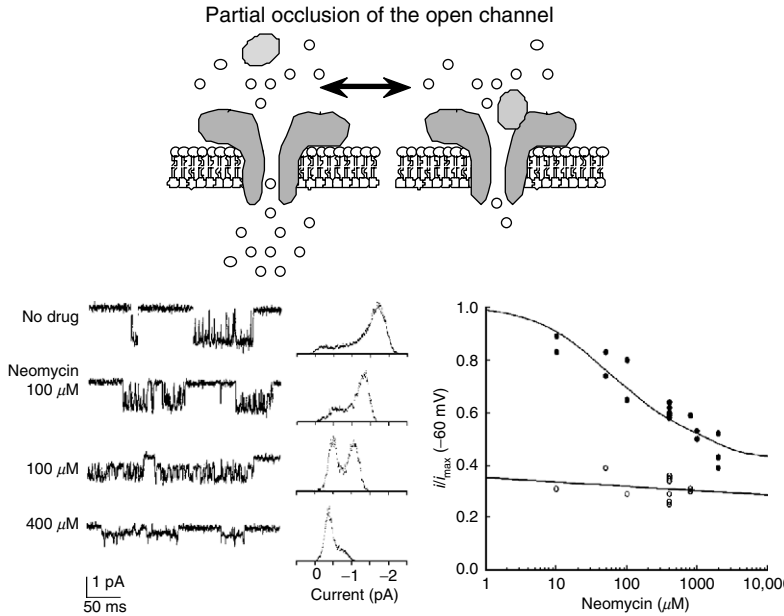

FIGURE 10 Block of MS channels by aminoglycoside antibiotics. (Top) Illustration showing the molecular interpretation of the partial occlusion blocking model used to describe the substrate blocking behavior. In this model, an aminoglycoside antibiotic can enter the channel conduction pathway; however, it only partially blocks the channel. (Bottom, right) Records showing the block of single MS channels with increasing concentrations of neomycin. Increasing the concentration of neomycin reduces the amplitude of the single-channel current and causes the transition of the channel to a level that is ~40% of the fully open level. The amplitude distribution of the open channel current is shown at the right of the records. There is a progressive reduction in the amplitude of the fully open state and a parallel occupancy of the subconductance level. (Bottom, left) Concentration dependence of the reduction of the single-channel current by neomycin. The amplitude of the single-channel current in the presence of drug is normalized to that in the absence of drug (i/imax) for the full conductance state (filled symbols) and the subconductance state (open symbols). The smooth curve drawn through the open symbols is the fit to a model in which drug binding to a single site is modified by the presence of fixed negative charges. Holding potential was −60 mV. Adapted from Winegar *et al.* (1996).

MS channels in FDB fibers by neomycin. Increasing the concentration of neomycin had two effects that occurred in parallel: it reduced the amplitude of the single-channel current and caused the channel to occupy a subconductance state of approximately one-third the amplitude of the fully open channel. Analysis of the blocking mechanism suggested that only one of the positively charged amino groups on the aminoglycoside molecule entered into the channel pore.

VII. CONCLUSIONS

Dystrophin-deficient muscle shows characteristic cytoskeletal abnormalities relevant to understanding MS channel gating behavior. Ultrastructural studies show that the absence of dystrophin is associated with irregularities of the spectrin cytoskeleton (Williams and Bloch, 1999a,b). For example, there are regions in which spectrin is lost over M lines and in longitudinal strands that leaves discrete areas of the plasma membrane without structural support from the cytoskeleton. We suspect that mechanical disturbances would likely cause changes in membrane composition or structure at such sites, and such changes could underlie the gating mode shifts in dystrophin-deficient muscle. The localization of spectrin abnormalities to discrete surface domains would be consistent with the observation of gating mode conversion at only a fraction of the recording sites.

A switch in MS channel gating from SA to SI has been described for MS channel in other systems, notably Shaker K^+ channels (Gu *et al.*, 2001) and gramacidin A channels incorporated into pure lipid membranes (Martinac and Hamill, 2002). Any number of mechanisms could account for shifts between SA and SI gating but recent work has focused on changes in the extent of hydrophobic mismatch between the bilayer and exterior hydrophobic length of the channel protein, which can influence ion channel conformational state (Cantor, 1994, 1999; Lundbaek and Andersen, 1994). In particular, a change in bilayer thickness that results from accumulation of lipids with longer or shorter acyl chain lengths relative to the embedded channel length can account for the key features of SA and SI gating in *mdx* muscle (Martinac and Hamill, 2002).

The model assumes that channels open when hydrophobic mismatch is minimal. If bilayer thickness is greater than the channel hydrophobic length, membrane stretch would cause the bilayer to thin, thus reducing the mismatch, and produce SA gating. This transduction process would occur primarily in wild-type muscle, but also in some patches on *mdx* muscle. A shift to the SI gating mode would occur when there is a change in local lipid composition near the channel that reduces hydrophobic mismatch.

A reduced mismatch favors opening and channels would remain open in the absence of a pressure stimulus. SI gating occurs since membrane stretch causes bilayer thinning and increased mismatch. Although a change in hydrophobic mismatch provides a simple model for explaining the complex changes in MS channel gating in *mdx* muscle, the dystrophin-dependent processes that control bilayer composition and/or thickness are not known.

The molecular identity of the MS channel in skeletal muscle is not known. Recent work has indicated that skeletal muscle expresses several members of the TRPC and TRPV channel families, including TRPC1, TRPC4, TRPC6 (Vandebrouck *et al.*, 2002), and TRPV2, TRPV3, TRPV4, and TRPV6 (Krüger *et al.*, 2004). The conductance and selectivity of MS channels in skeletal muscle fall within the range of those for known TRP channels. Several of the TRP channels that are expressed in skeletal muscle are thought to be MS channels including TRPV2 (Iwata *et al.*, 2002), TRPV4 (Liedtke, 2005), and TRPC1 (Maroto *et al.*, 2005). A future goal will be to understand the functional diversity of MS channels in skeletal muscle using transgenic and small interfering RNA methods.

References

Adams, M. E., Butler, M. H., Dwyer, T. M., Peters, M. F., Murnane, A. A., and Froehner, S. C. (1993). Two forms of mouse syntrophin, a 58 kd dystrophin-associated protein, differ in primary structure and tissue distribution. *Neuron* **11,** 531–540.

Ahn, A. H., Freener, C. A., Gussoni, E., Yoshida, M., Ozawa, E., and Kunkel, L. M. (1996). The three human syntrophin genes are expressed in diverse tissues, have distinct chromosomal locations, and each bind to dystrophin and its relatives. *J. Biol. Chem.* **271,** 2724–2730.

Brehm, P., Kullberg, R., and Moody-Corbett, F. (1984). Properties of non-junctional acetylcholine receptor channels on innervated muscle of *Xenopus laevis*. *J. Physiol.* **350,** 631–648.

Cantor, R. S. (1999). Lipid composition and the lateral pressure profile in bilayers. *Biophys. J.* **76**(5), 2625–2639.

Eisenman, G. (1962). Cation selective glass electrodes and their mode of operation. *Biophys. J.* **2,** 259–323.

Ermakov, Yu., A., Averbakh, A. Z., Arbuzova, A. B., and Sukharev, S. I. (1998). Lipid and cell membranes in the presence of gadolinium and other ions with high affinity to lipids. 2. A dipole component of the boundary potential on membranes with different surface charge. *Membr. Cell Biol.* **12**(3), 411–426.

Ervasti, J. M., and Campbell, K. P. (1993). A role for the dystrophin-glycoprotein complex as a transmembrane linker between laminin and actin. *J. Cell. Biol.* **122**(4), 809–823.

Ervasti, J. M., Ohlendieck, K., Kahl, S. D., Gaver, M. G., and Campbell, K. P. (1990). Deficiency of a glycoprotein component of the dystrophin complex in dystrophic muscle. *Nature* **345**(6273), 315–319.

Franco, A., Jr., and Lansman, J. B. (1990a). Stretch-sensitive channels in developing muscle cells from a mouse cell line. *J. Physiol.* **427,** 361–380.

Franco, A., Jr., and Lansman, J. B. (1990b). Calcium entry through stretch-inactivated ion channels in *mdx* myotubes. *Nature* **344,** 670–673.

Franco, A., Jr., Winegar, B. D., and Lansman, J. B. (1991). Open channel block by gadolinium ion of the stretch-inactivated ion channel in *mdx* myotubes. *Biophys. J.* **59**(6), 1164–1170.

Franco-Obregón, A., Jr., and Lansman, J. B. (1994). Mechanosensitive ion channels in skeletal muscle from normal and dystrophic mice. *J. Physiol.* **481,** 299–309.

Franco-Obregón, A., and Lansman, J. B. (2002). Changes in mechanosensitive channel gating following mechanical stimulation in skeletal muscle myotubes from the *mdx* mouse. *J. Physiol.* **539,** 391–407.

Gu, C. X., Juranka, P. F., and Morris, C. E. (2001). Stretch-activation and stretch-inactivation of Shaker-IR, a voltage-gated K^+ channel. *Biophys. J.* **80**(6), 2678–2693.

Guharay, F., and Sachs, F. (1984). Stretch-activated single ion channel currents in tissue-cultured embryonic chick skeletal muscle. *J. Physiol.* **352,** 685–701.

Haws, C. M., Winegar, B. D., and Lansman, J. B. (1996). Block of single L-type Ca^{2+} channels in skeletal muscle fibers by aminoglycoside antibiotics. *J. Gen. Physiol.* **107**(3), 421–432.

Hoffman, E. P., Brown, R. H., Jr., and Kunkel, L. M. (1987). Dystrophin: The protein product of the Duchenne muscular dystrophy locus. *Cell* **51,** 919–928.

Ibraghimov-Beskrovnaya, O., Ervasti, J. M., Leveille, C. J., Slaughter, C. A., Sernett, S. W., and Campbell, K. P. (1992). Primary structure of dystrophin-associated glycoproteins linking dystrophin to the extracellular matrix. *Nature* **355,** 696–702.

Ibraghimov-Beskrovnaya, O., Milatovich, A., Ozcelik, T., Yang, B., Koepnick, K., Francke, U., and Campbell, K. P. (1993). Human dystroglycan: Skeletal muscle cDNA, genomic structure, origin of tissue specific isoforms and chromosomal localization. *Hum. Mol. Genet.* **2,** 1651–1657.

Iwata, Y., Katanosaka, Y., Arai, Y., Komamura, K., Miyatake, K., and Shigekawa, M. (2002). A novel mechanism of myocyte degeneration involving the Ca^{2+} permeable growth factor-regulated channel. *J. Cell Biol.* **161**(5), 957–967.

Koenig, M., Monaco, A. P., and Kunkel, L. M. (1988). The complete sequence of dystrophin predicts a rod-shaped cytoskeletal protein. *Cell* **53**(2), 219–226.

Krüger, J., Kunert-Keil, C., and Brinkmeir, H. (2004). RNA transcripts coding for members of the TRP cation family in mouse skeletal and heart muscle. *Deutsche Physiol. Gessel. Abstracts.*

Liedtke, W. (2005). TRPV4 plays an evolutionary conserved role in the transduction of osmotic and mechanical stimuli in live animals. *J. Physiol.* **567**(Pt. 1), 53–58.

Lundbaek, J. A., and Andersen, O. S. (1994). Lysophospholipids modulate channel function by altering the mechanical properties of lipid bilayers. *J. Gen. Physiol.* **104**(4), 645–673.

Maroto, R., Raso, A., Wood, T. G., Kurosky, A., Martinac, B., and Hamill, O. P. (2005). TRPC1 forms the stretch-activated cation channel in vertebrate cells. *Nat. Cell. Biol.* **7**(2), 179–185.

Martinac, B., and Hamill, O. P. (2002). Gramicidin A channels switch between stretch activation and stretch inactivation depending on bilayer thickness. *Proc. Natl. Acad. Sci. USA* **99**(7), 4308–4312.

Pasternak, C., Wong, S., and Elson, E. L. (1995). Mechanical function of dystrophin in muscle cells. *J. Cell Biol.* **128,** 355–361.

Sicinski, P., Geng, Y., Ryder-Cook, A. S., Barnard, E. A., Darlison, M. G., and Barnard, P. J. (1989). The molecular basis of muscular dystrophy in the *mdx* mouse: A point mutation. *Science* **244,** 1578–1580.

Vandebrouck, C., Martin, D., Colson-Van Schoor, D., Debaix, H., and Gailly, P. (2002). Involvement of TRPC in the abnormal calcium influx observed in dystrophic (*mdx*) mouse skeletal muscle fibers. *J. Cell Biol.* **158**(6), 1089–1096.

Williams, M. W., and Bloch, R. J. (1999a). Extensive but coordinate reorganization of the membrane skeleton in myofibers of dystrophic (mdx) mice. *J. Cell. Biol.* **144**(6), 1259–1270.

Williams, M. W., and Bloch, R. J. (1999b). Differential distribution of dystrophin and beta-spectrin at the sarcolemma of fast twitch skeletal muscle fibers. *J. Muscle Res. Cell Motil.* **20**(4), 383–393.

Winegar, B. D., Haws, C. M., and Lansman, J. B. (1996). Subconductance block of single mechanosensitive ion channels in skeletal muscle fibers by aminoglycoside antibiotics. *J. Gen. Physiol.* **107**(3), 433–443.

Yang, X. C., and Sachs, F. (1989). Block of stretch-activated ion channels in *Xenopus* oocytes by gadolinium and calcium ions. *Science* **243,** 1068–1071.

Yoshida, M., and Ozawa, E. (1990). Glycoprotein complex anchoring dystrophin to sarcolemma. *J. Biochem.* (*Tokyo*) **108**(5), 748–752.